

Enhancing the Hardness and Wear Resistance of AA5052 by Reinforcing with Alumina and Bauxite Natural Particles

Sattar Hantosh A. Alfatlawi^{1,2}, Fatma Hentati^{3*}, Neila Masmoudi Khabou¹

¹ *Electromechanical Systems Laboratory (LASEM), National Engineering School of Sfax, University of Sfax, Tunisia BP 1173 3038*

² *College of Material's Engineering, University of Babylon, Iraq.*

³ *Applied Mechanics and Engineering Laboratory (LR-MAI), National Engineering School of Tunis ENIT, Tunis, 1002, Tunis*

Received 21 Jul 2024

Accepted 25 Nov 2024

Abstract

Waste cables represent a significant source of raw materials, particularly metals, necessitating their economic and ecological recovery. This study focuses on the recovery of aluminum from waste cables and explores the use of cost-effective natural ceramics as replacements for expensive ceramic materials in reinforcement applications. Initially, Aluminum Alloy (AA5052) was prepared, followed by the production of two types of composite materials: one incorporating 7 wt% alumina particles (30±5 nm) and another 7 wt% bauxite particles (0.98 μm) as natural ceramic additives.

Experimental investigations focused on mechanical and physical characteristics, such as wear rate, hardness, and microstructural analysis using scanning electron microscopy (SEM), energy dispersive spectroscopy (EDS), and X-ray diffraction (XRD). The findings reveal significant improvements in hardness and wear resistance with the addition of alumina and bauxite reinforcements, specifically alumina enhanced hardness by 48%, while bauxite demonstrated a 56% improvement. Both materials reduced wear rates by approximately 55% for time periods and exhibited consistent performance over extended durations. Importantly, the comparable effects of alumina and bauxite on product properties indicate that bauxite can effectively replace advanced ceramic materials in composite reinforcements, offering promising opportunities for cost reduction across various applications.

© 2025 Jordan Journal of Mechanical and Industrial Engineering. All rights reserved

Keywords: Aluminum Alloy (AA5052), Nano-composite, Alumina, Bauxite, Stir casting process, Wear Rate, Hardness.

1. Introduction

The lightweight and unique properties of aluminum, have contributed to its widespread usage across numerous fields in recent years. Its other most important characteristics, such as high electrical and thermal conductivity and corrosion resistance. Furthermore, Aluminum can be manufactured inexpensively using a variety of production methods. Despite its high specific strength, Aluminum exhibits poor performance at high temperatures. Due to attributable to its low melting point, thermal and electrical properties, low hardness, and extremely low wear resistance. Although, aluminum and its alloys stand out as the most commonly used matrix materials in the production of metal matrix composites. [1, 2].

Recycling of scrap is accompanied by problems, including sorting impurities, to overcome this problem, dilution and reduction techniques are used. In addition to modern methods, including water jets, cameras equipped with sensors, magnets, and others. Treating scrap impurities, cutting, and sorting is important for the success the recycling process. The choice of manufacturing

methods for aluminum compounds and the selection of appropriate raw materials are crucial factors according intended applications. Titanium diboride (TiB₂) was used to reinforce the 5052A alloy by stir casting to fabricate a composite material. The weight ratios of reinforcement (2.5, 5 and 7.5 wt. %) were mixed. The result was an improvement in hardness (30%) and wear resistance (36%) with high load. The sliding speed (1 m/s and 3 m/s) and load (10 N and 50 N) to determine the wear resistance [3-5].

In general, aluminum alloys especially alloys that contain magnesium such as alloy AA5052, have become highly demanded. Thus, these alloys have many applications in various fields, that due to their distinctive properties. Therefore, can be see their presence in the fields of marine industries, shipbuilding, aviation, space industries, and others. In other words, fields that require strength with light weight, which improves speed and thus reduces fuel. In some cases, it is necessary to add materials as reinforcements to improve the properties of these alloys, including ceramic materials. Among these properties are wear resistance, high hardness and others, that are obtained after reinforcing aluminum alloys with ceramic materials. [6-9].

* Corresponding author e-mail: fatma.hentati1@gmail.com.

Due to their distinctive mechanical and frictional properties, aluminum alloys such as (AA6063 and AA5052) reinforced with ceramic particles find wide application in various engineering fields. Therefore, the choice of the stir casting method is the most suitable for these alloys that are reinforced with silicon nitride (Si_3N_4), aluminum nitride (AlN), Boron Carbide (B_4C) and titanium carbide (TiC) [10-12].

Stir casting used to manufacture a composite material from aluminum alloy (AA6063) and strengthened by (Nano AlN) with weight mixing ratios (4, 8, and 12 wt.%). Then, the mechanical and physical properties of the product were examined, and the results were satisfactory. The SEM, hardness, wear, tensile, yield strength, flexural strength, compression, electrical conductivity etc. The additions are ceramic materials in different proportions to achieve the desired. Aluminum alloy AA5052 containing (Mg 2.5%, Cr 0.25%, Si 0.2%, Zn 0.1%, Cu 0.1%, Fe 0.35%, and balance of aluminum) was strengthened with boron carbide particles and mixing ratio (5 wt.% B_4C), that, has high stiffness and modulus of elasticity. Stir casting is used to prepare the composite, that cost effective method for ceramic composite materials [13-15].

Furthermore, aluminum alloy (AA5052) reinforced first with zirconium oxide and then with alumina, each with varying addition ratios through the stir casting method. A stir casting (600–800 rpm) used to manufacture the composite material based on alloy AA5052 and reinforced with alumina (5wt.% and 10wt.%) and zirconium oxide (8wt.%). The wear resistance conducted with three levels and three load values (20, 25, and 30 N), so the velocity of sliding (300, 400, and 500 rpm) selected. The lowest wear rate was achieved under specific conditions: a load of 25 N, a sliding speed of 300 r/min, and a 5% addition ratio. In contemporary industries, the evolution of materials is indispensable, and among them, metal matrix composites stand out as crucial. Their distinctive properties make them one of the most significant materials in modern industry [16, 17].

Several researchers have shown that the effect of ceramic materials such as (SiC) was clear in improving the mechanical properties as well as the ease of manufacturing. The effect on wear resistance, strength, cohesion in the structure and all mechanical properties was clear. Recently, aluminum-based composites and its alloys have a prominent presence in the industry in all fields.

[18–20], have observed improvements in hardness, density, and porosity reduction in samples incorporating sea sand. Additionally, alternative natural materials, like agricultural waste such as rice husks, have been explored. These materials closely resemble traditional options like alumina, displaying attributes such as lightweight, wear resistance, and various thermal, mechanical, and physical properties. Importantly, their cost-effectiveness in production has yielded comparable results to those achieved with traditional additives.

Further studies [21-23] support the efficacy of incorporating natural materials, such as bauxite, resulting in increased density and reduced porosity. This, in turn, enhances the thermal properties alongside other notable improvements. Bauxite, known for its role in aluminum production, also serves as a raw material for alumina, offering commendable thermal and chemical stability at elevated temperatures. Its excellent wear resistance and hardness becomes evident in the enhanced hardness. Also, modulus of elasticity, and fracture toughness when introducing Iraqi bauxite at 2 and 4 wt. %. However, it's worth noting that at 6 wt. %, there is a reduction in fracture toughness attributed to the brittle behavior of aluminum composite materials.

From previous studies, it can be concluded that the alloy (AA5052) has taken a large space application after being reinforced with different materials. Thus, the reinforcements are synthetic ceramic materials, and the aluminum used as a matrix to obtain a high strength-to-weight ratio. In this study, the economic cost of composite material based on Al5052 has been reduced. This cost reduction achieved by providing the matrix from recycled aluminum, and substituting expensive ceramic (Al_2O_3) with natural (Bauxite), that cost-effective alternative.

2. Experimental Set up

2.1. Material preparation

The preparation of samples for the AA5052 alloy according ASTM (B209), and additive materials followed a specific procedure. Initially, aluminum waste was melted at 675 °C in a graphite melting pot that inside the furnace in furnace (Figure 1), until the slag appeared on the surface of the molten metal.



Figure 1. Furnace of melting

The chromium powder, covered with aluminum foil, was heated to 150°C, then immersed under the slag at a ratio of 0.25%. Additionally, a strip of magnesium, covered with aluminum foil at a ratio of 2.5%, was added and immersed under the slag. The aluminum and magnesium completely melted, while the chromium atoms as form nucleation centers during the cooling. The molten were mixed using an electric mixer at a speed of 700 rpm. To aid in slag removal, aqueous aluminum chloride (AlCl₃.6H₂O) was added and thoroughly mixed, resulting in successful slag removal. The molten mixture was then poured into a preheated metal mold at 250°C, see Figure 2.

After solidification and cooling at room temperature, the AA5052 alloy sample was obtained. See Figure 3. The chemical compositions of AA5052 in weight percent, of this material are given in Table 1.

To generate the new sample types, the preceding steps used to produce the AA5052 alloy were reiterated, until

the pouring temperature is reached (675 °C). Thus, choosing weight percentage (6%, 7% and 8%), where 6% were evident casting mistakes, that were visually detected. The percentage 8% gave a higher hardness than 7%, but increased brittleness and presence of agglomeration, that leads to vibrations during cutting or machining. That leads to cracks in the surface, so ratio (7 %) was chosen. The alpha-type Nano-alumina (Figure 4), at a ratio of (7 wt. %) was heated to 150 °C, the molten temperature was elevated more than liquid temperature to 800°C.

Then, cooled at 600 °C, the preheated alumina particles are added with manual mixing of semi liquid for three minutes. That was to improve the wettability and adhesion of the matrix liquid to the alumina particle surface. After that the molten temperature is raised to 800 °C with good stirring at 700 rpm.



Figure 2. Casting die

Table 1. Chemical composition of AA5052 (in wt.%) [14]

Mg	Fe	Cu	Mn	Si	Zn	Ti	B	V	Cr	Al
2.5	0.4	0.12	0.1	0.25	0.15	0.1	0.05	0.1	0.25	Balance



Figure 3. Samples prepared by stir casting



Figure 4. Samples materials

Then, cooled at 600 °C, the preheated alumina particles are added with manual mixing of semi liquid for three minutes. That was to improve the wettability and adhesion of the matrix liquid to the alumina particle surface. After that the molten temperature is raised to 800°C with good stirring at 700 rpm. The molten mixture was poured into the preheated mold at (250 °C), to create the first sample of the aluminum matrix composite. To prepare the last samples with same addition, (7 wt.%) of bauxite (Figure 4) with a size of 0.98 μm , were fired at 1450°C to eliminate moisture and impurities. The preceding steps were used to produce alumina samples. The additional samples were obtained using bauxite, the casting of all sample types was completed. Following the casting processes, and to further enhance the homogeneity of the samples, a homogenization process was carried out after completing the casting operations. Once the furnace temperature reached 500°C, the samples were placed inside the furnace for 3 hours. Subsequently, the samples were removed and allowed to cool at room temperature.

2.2. Tests Methods

Subsequently, the samples underwent a testing process that included scanning electron microscopy (SEM), energy dispersive spectroscopy (EDS), X-Ray Diffraction (XRD), hardness, and wear rate assessments. In this study, an effort was made to address the cost factor for matrix by recycling of aluminum scrap, as well as the expensive advanced ceramic additives by substituting them with natural ceramic additives (bauxite), which is very cheap. This substitution was carried out under identical working methods, conditions, and addition ratios. Subsequently, the same tests were conducted to compare the results. Alumina, representing a conventional advanced ceramic material, was selected for comparison with Bauxite. It's worth noting that Bauxite typically contains a percentage of 60.46% of alumina, as indicated in Table 2, with the burnt type containing approximately 75%.

Table 2. Chemical composition of Bauxite in wt.% before burned.

Al ₂ O ₃	SiO ₂	Fe ₂ O ₃	TiO ₂	Others
60.46	12	8.56	1.05	17.93

The necessary test samples were precisely cut using a lathe machine, ensuring dimensions aligned with the specified requirements for the investigation. Subsequently, different types of aluminum oxide papers were utilized in the grinding and polishing processes. Following these preparations, the surfaces underwent treatment with an etching solution. Thermo Scientific Axia device is used for microstructure testing, SEM (Scanning Electron Microscope), and EDX (Energy Dispersive X-ray Spectroscopy) analysis was performed. For crystalline analysis, samples of the base alloy, the composite material of the alloy and alumina. Also, the alloy and bauxite were examined using an X-ray diffraction device (XRD 6000, Japan). Hardness tests were carried out according ASTM E10 using a Brinell device (Wilson/REICHERTER UH250) with 2.5mm/31.25 KPa. Three to five readings, each lasting 10 seconds, were taken, and an average was subsequently calculated. The wear rate conducted at (ASTM G99-17) and parameters are selected according to previous studies [5,7,9,17 and 27], using a Microtest MT4003/BIJUR device at various durations (10, 20, and 30 minutes), applying a selected force of 5 Newtons and a rotational speed of 250 rpm. The results for hardness and wear rate are illustrated in Figures 15 and 19, respectively.

3. Results and Discussions

3.1. Microscopic characterization

3.1.1. SEM Test

Figure 5 displays the SEM image of the alloy and composite material microstructure after homogenization at 500 °C. Figure 5(a) indicates the microstructure of the matrix, consisting of 2.5 wt.% magnesium, 0.25 wt.% chromium, with aluminum constituting the balance. Solidification initiates after the release of fusion heat, occurring below the melting point (T_m), and nucleation

begins. In this structure, the grain boundaries of chromium serve as nucleation centers. Subsequently, dendrites begin to form after the gathering of Al and Mg atoms, and grain growth continues until complete crystallization. Therefore, if another substance with a higher melting point than magnesium was present, the grains would hinder the growth of dendrites, as depicted in the other images (b and c).

Figure 5(b) shows the microstructure after adding the alumina particles to alloy. Thus, the image has more nucleation centers than the previous image (a), due to the addition of alumina particles. In other words, the results in an increased number of nucleation sites, which then grow into grains during melt solidification. In addition, good mixing, thermal homogenization, and heating of the particles before adding lead to a clear improvement in the microstructure. That means the process reduced the particle segregation or agglomeration due to the stirring and preheating of the particles before adding. Additionally, the alumina particles cause an obstruction to the growth of dendritic branches, which leads to obtaining a homogeneous and refined structure.

Figure 5(c), shows the presence of bauxite particles as reinforcement, that induces changes and refinement in the microstructure. Thus, as the image shows, there is shift towards more homogeneous grains, influenced by the presence of bauxite particles, good stirring, and thermal homogenization. Consequently, there is a noticeable reduction or elimination of dendrites, indicating a more homogeneous structure than that observed in (a) and (b).

As well as, the dendrite breakage caused by bauxite or obstruction of the growth of dendritic leads to refining the structure. Furthermore, there is no agglomeration due to preheating the bauxite particles before they're added to the molten mixture. Thus, it can be concluded that the sample resulting from the addition of bauxite gives a more homogeneous structure than the sample reinforced with alumina.

Overall, the microstructure depicted across the figures appears homogeneous, reflecting effective mixing facilitated by the electric mixer during the stir casting process. Additionally, the use of a cast iron mold, which maintains temperature stability for an extended period, and the employment of suitable raw materials contribute to this homogeneity. The presence of magnesium is crucial in all composites to enhance wetting, promoting cohesion between the matrix and the reinforcement particles. Furthermore, the introduction of magnesium as a wetting agent during alloy casting ensures the uniform distribution of reinforcement particles [24]

Occasionally, SEM test micrographs reveal the presence of black spots in certain areas, indicating the agglomeration of added particles due to the density difference between the matrix and the reinforcements. Consequently, during solidification, dendrites of the aluminum alloy initiate solidification, hindering the progress of reinforcement particles at the solid-liquid interface. This results in the segregation of reinforcement particles within the internal dendrite [24].

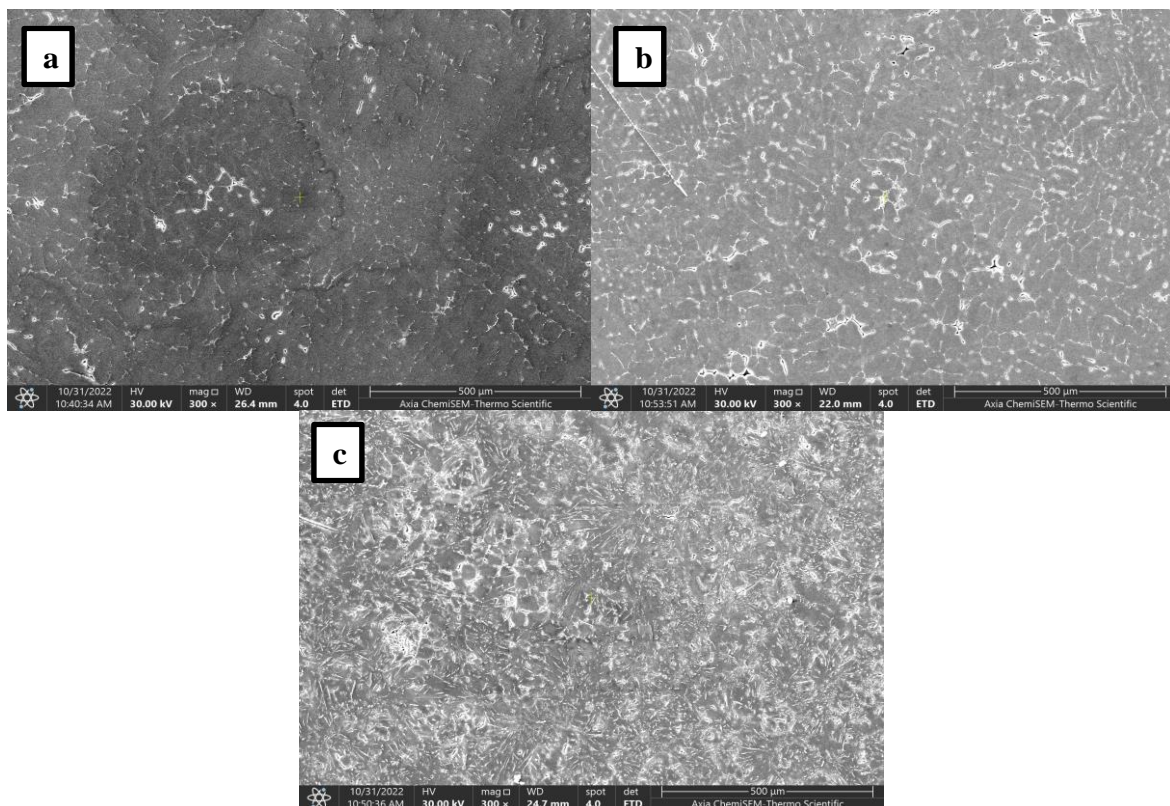


Figure 5. SEM micrographs: (a) AA5052, (b) AA5052+ Al₂O₃ and (c) AA5052+ Bauxite.

3.1.2. EDS Test

EDS technique complements SEM inspection, and is conducted to confirm the presence of additives at all casting stages. The results of the EDS examination are presented in the following figures and tables, focusing on selected areas of the sample.

The images depicted in Figure 6 represent the element distribution in AA5052. Specifically, Figures 6(a), (b), and (c) illustrate the presence of the main elements (Aluminum, Magnesium, and Chromium) in AA5052, respectively. Figure 7 provides the map data of Aluminum, Magnesium, and Chromium in AA5052, which

corroborates the findings from Figure 6 and Table 7. The atomic and weight percentages along with the percentage error in the Alloy AA5052 structure are depicted in Table 3. Hence, the presence of the main elements constituting the alloy is observed, with minor variations in the values of these elements.

This phenomenon can be attributed to losses incurred during slag removal, as well as the effects of reactions and evaporation, compounded by the presence of impurities. This is further elucidated in the subsequent EDS test tables of composite materials. Additionally, variations in percentages may occur when different areas are selected for examination.

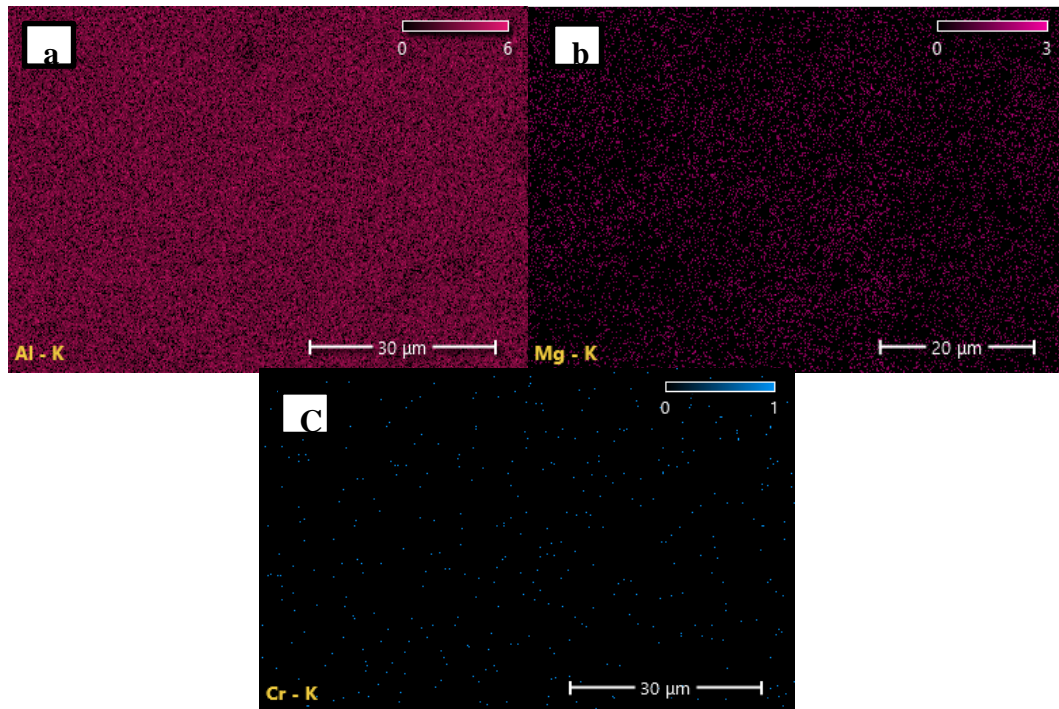


Figure 6. EDS elemental distribution Images for AA5052: (a) Al, (b) Mg, and (c) Cr.

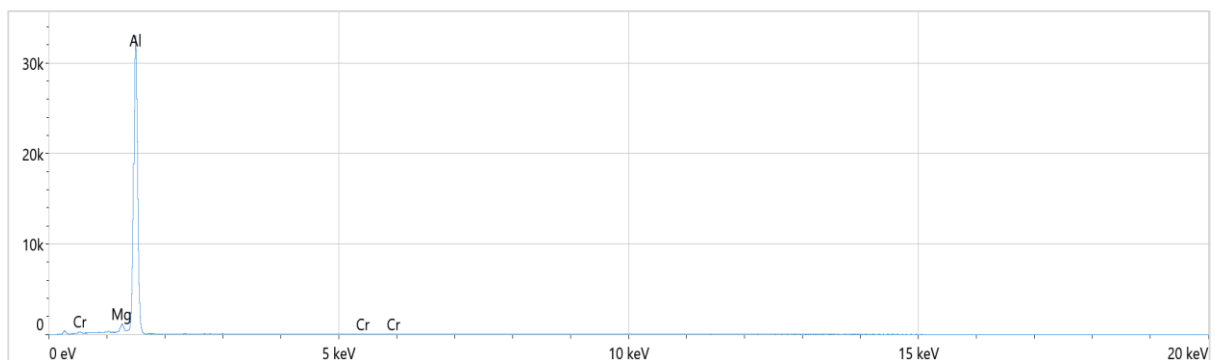


Figure 7. Map data of elementals presence for AA5052.

Table 3. Elements percentage in the alloy AA5052 structure.

Element	Atomic %	Atomic % Error	Weight %	Weight % Error
Mg	1.9	0.1	2.1	0.1
Al	97.92	0.4	97.93	0.4
Cr	0.18	0.1	0.17	0.1

Figure 8(a, b, c, and d) depict the distribution of elements (Al, O, Mg and Zn) in the microstructure of aluminum alloy reinforced with alumina.

Hence, the presence of Aluminum (Al) and Oxygen (O) confirms the presence of Al₂O₃ in the alloy. Additionally, the presence of Aluminum (Al) and Magnesium (Mg) indicates the presence of AA5052. The absence of Chromium in this selected area is attributed to its small quantity in the sample. Furthermore, a small percentage of Zinc is observed, which is considered one of the impurities associated with aluminum oxide.

Figure 9 provides the map data of Aluminum (Al), Oxygen (O), Magnesium (Mg), and Zinc (Zn) in AA5052 + Al₂O₃. Table 4 displays the atomic and weight percentages along with the percentage error in the structure of AA5052 + Al₂O₃. Therefore, the presence of the main elements contained in the composite materials reinforced with alumina can be observed in Figures 8 and 9, as well as Table 4, with minor deviations from the expected values.

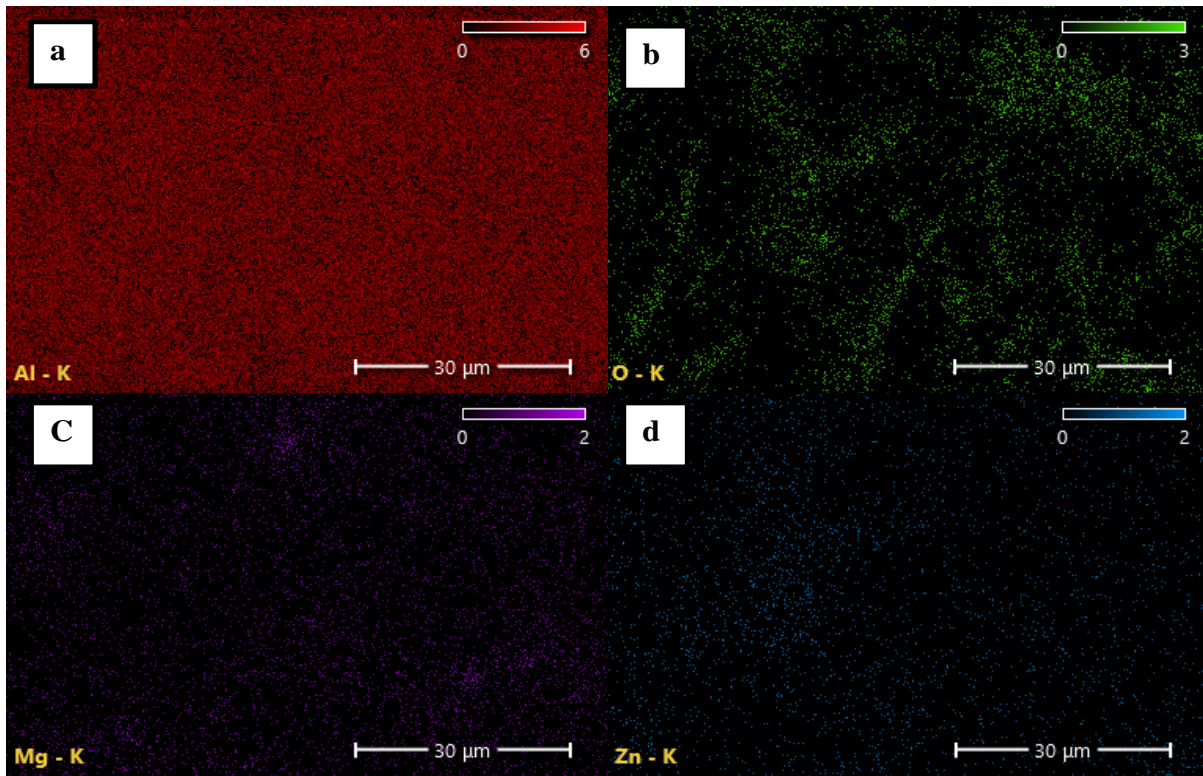


Figure 8. EDS Elemental Distribution Images for AA5052+ Al₂O₃: (a) Al, (b) O, (c) Mg, and (d) Zn.

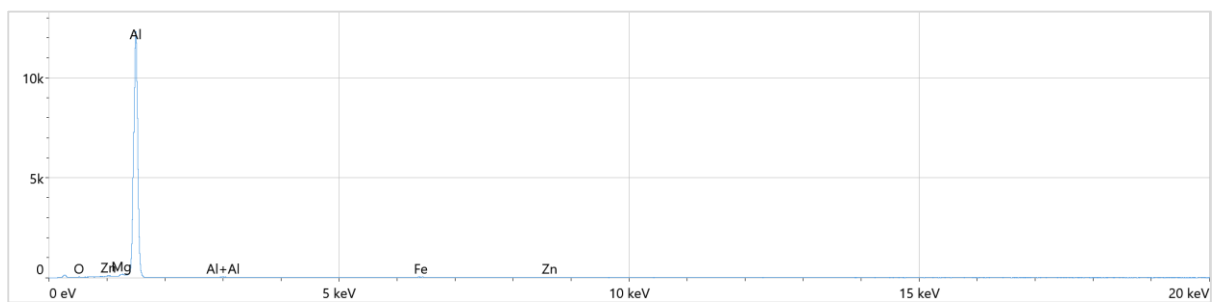


Figure 9. Map data of elements presence for AA5052+Al₂O₃.

Table 4. Elements percentage in the composite AA5052+Al₂O₃ Structure.

Element	Atomic %	Atomic % Error	Weight %	Weight % Error
O	4.5	0.3	5.1	0.2
Mg	0.8	0.1	1.1	0.1
Al	94.5	0.4	93.7	0.4
Zn	0.2	0.1	0.1	0.1

Indeed, these deviations can be attributed to losses during slag removal, reactions, evaporation effects, and the presence of impurities. Additionally, the largest peak observed typically represents the highest percentage of aluminum.

Figure 10 provides the map data of Aluminum (Al), Oxygen (O), Magnesium (Mg), Iron (Fe), Manganese (Mn), and Titanium (Ti) in AA5052 + bauxite, as confirmed by Figure 11 and Table 5. This indicates the presence of basic elements such as Aluminum and Oxygen, along with additional elements including Manganese, Iron, and Titanium in this composite material of AA5052 + bauxite.

The final set of images, Figure 11 (a, b, c, d, e, f), displays the distribution of elements in the alloy after the addition of bauxite. This highlights the presence of elements such as Aluminum (Al), Oxygen (O), Magnesium (Mg), Iron (Fe), Manganese (Mn), and Titanium (Ti) in the aluminum alloy reinforced by bauxite (AA5052 + Bauxite).

Table 5 presents the atomic and weight percentages along with the percentage error in the structure of Alloy AA5052 + bauxite. Therefore, the basic elements (Al, O, and Mg) can be observed in all figures and tables for the samples. Additionally, new elements such as manganese, iron, and titanium appear in the composite reinforced with bauxite, as bauxite contains these elements.

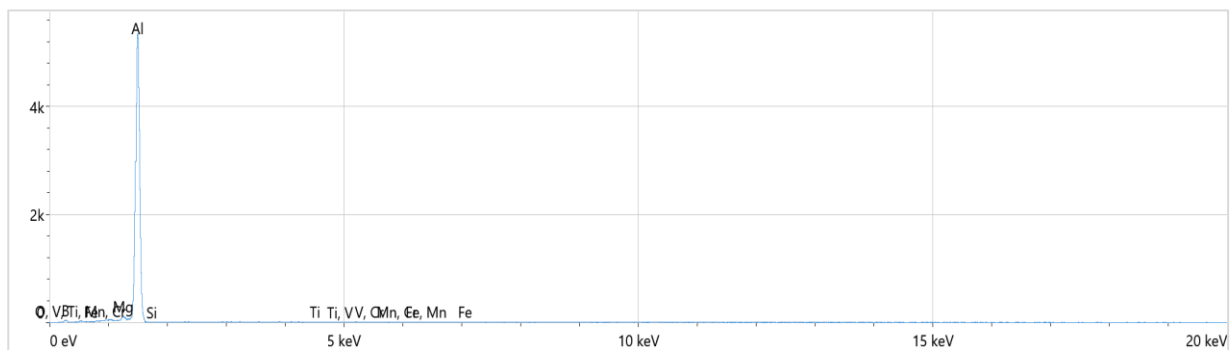


Figure 10. Map data of elementals presence for AA5052+Bauxite.

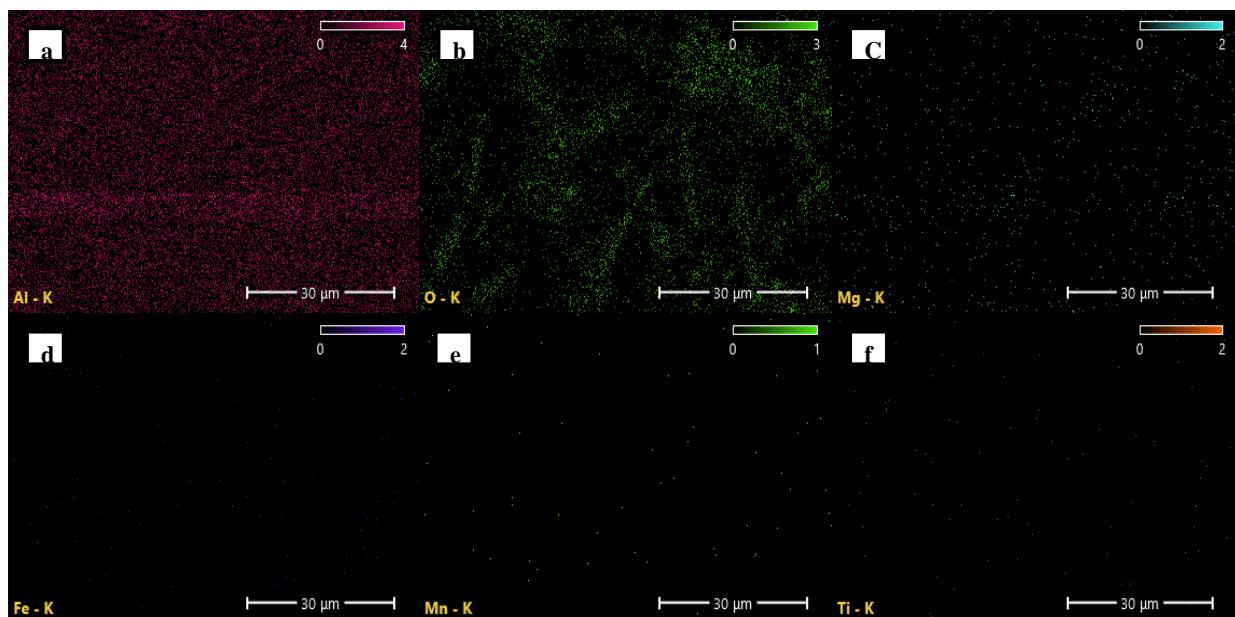


Figure 11. EDS Elemental distribution Images for AA5052+ Bauxite: (a) Al, (b) O, (c) Mg, (d) Fe, (e) Mn, and (f) Ti.

Table 5. Elements percentage in the composite AA5052+Bauxite structure.

Element	Atomic %	Atomic % Error	Weight %	Weight % Error
O	4.2	0.4	4.5	0.2
Mg	1.1	0.1	1.0	0.1
Al	94.4	0.5	93.7	0.5
Ti	0.0	0.0	0.1	0.1
Mn	0.1	0.1	0.3	0.2
Fe	0.2	0.1	0.4	0.2

3.1.3. X-Ray Diffraction measurements

Figures 12 and 13 present the XRD patterns at room temperature for the AA5052+ 7% Al₂O₃ particles mixture and AA5052+ 7% bauxite mixture, respectively. The sharp peaks observed in the patterns indicate the excellent crystallization of the composites. The XRD pattern in Figure 12 closely aligns with the reported values for aluminum-zinc (JCPDS, Card No. 00-052-0856) and magnesium (JCPDS, Card No. 01-089-7195). Notably, there is no discernible peak for chromium due to its low percentage (0.25%) within the AA5052 alloy.

Figure 13 depicts the phase analysis of the AA5052+7% bauxite mixture, closely aligning with comparative values for bauxite, particularly the gibbsite phase (JCPDS, Card No. 00-15-0776), and a limited presence of kaolinite (JCPDS, Card No. 01-080-0885). Notably, the major crystalline phase, characterized by extremely sharp peaks, is gibbsite, accompanied by a modest quantity of boehmite (JCPDS, Card No. 21-1307). These findings closely be similar to values associated with gibbsite, with certain peaks indicative of aluminum, consistent with (JCPDS, Card No. 04-0787).

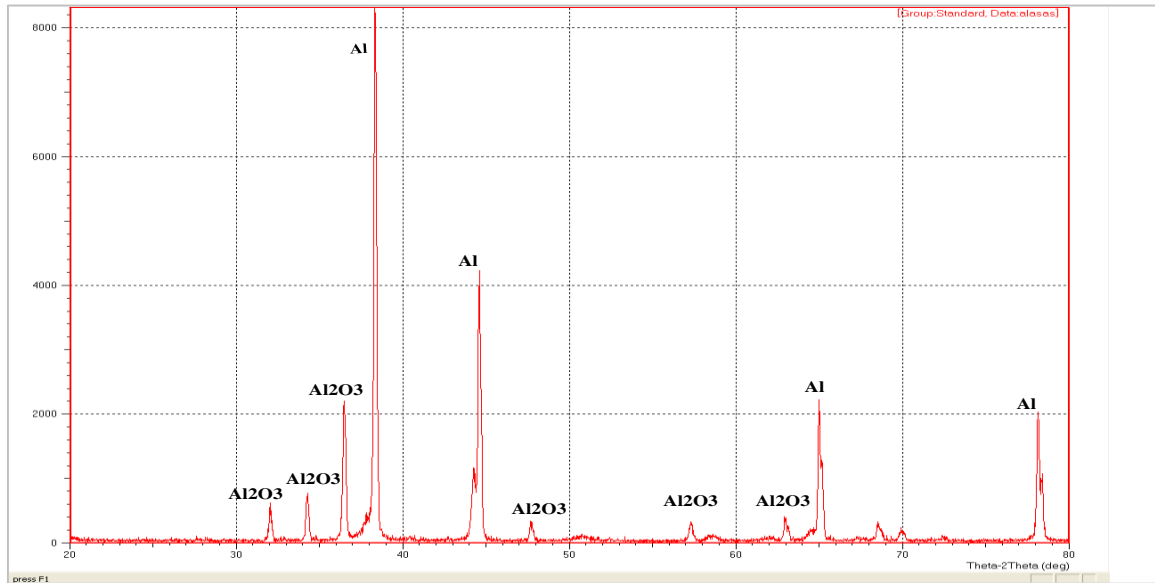


Figure 12. X-Ray Diffraction test (XRD) of AA5052+ 7% Al₂O₃.

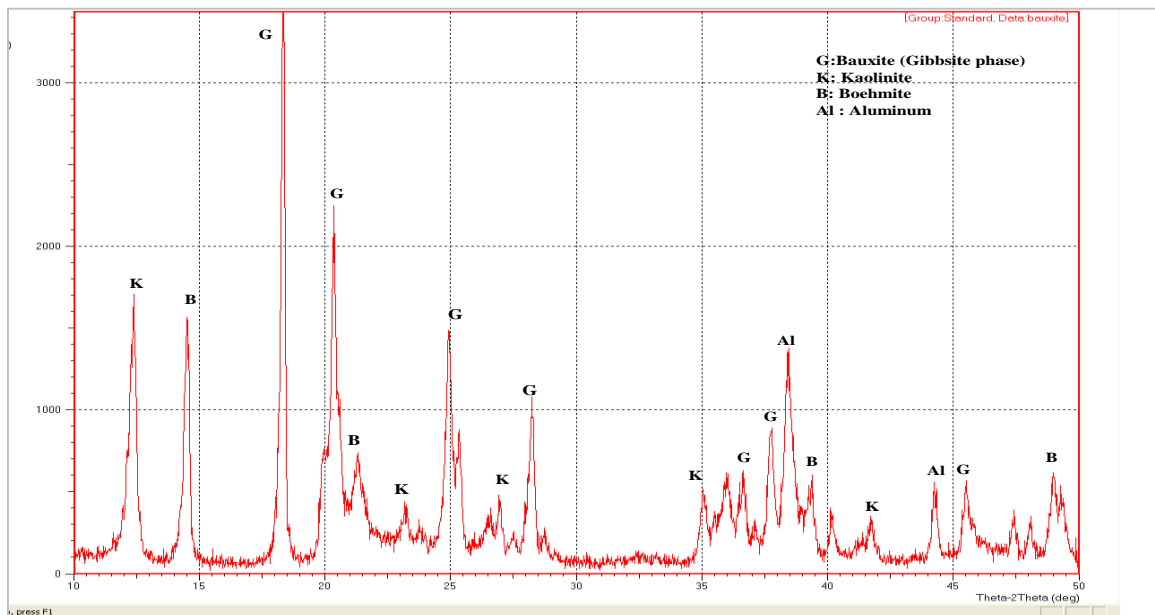


Figure 13. X-Ray Diffraction Test (XRD) of AA5052+7% Bauxite.

In general, the XRD figures (12, 13) affirm the presence of aluminum as a fundamental element, consistent with the findings from the EDS examination. Figure 12, wherein aluminum manifests as the highest peaks, additionally reveals the presence of aluminum oxide in the remaining peaks, indicating the structure of the composite reinforced with alumina. Figure 13, representing the composite material based on the alloy and reinforced with bauxite, exhibits a diverse array of elements. It is evident that various phases such as Gibbsite, Kaolinite, Boehmite, and aluminum are present, indicative of the constituent elements of bauxite. The (G) phase, representing bauxite, is predominant in most of the peaks, with the presence of kaolin evident in other peaks. Furthermore, enhancing the properties of the matrix results from various factors, including a homogeneous distribution. Like that, grain refinement, reduction of porosity, and improved interconnection between the matrix and reinforcements. Therefore, the homogeneous distribution of reinforcements increases interconnection, thereby improving mechanical properties[26].

In this regard, segregation of particles during solidification may arise due to density variations between the reinforcement and matrix. However, the incorporation of Nano-ceramic particles and increasing their percentages enhances mechanical properties while reducing defects[27,28]. Typically, when casting the matrix alone or with reinforcements, porosity is minimized by improving the wettability of preheated reinforcements before addition. This precaution ensures a strong bond between the matrix and reinforcements, mitigating challenges associated with the stir casting method. One such challenge during liquid mixing is the agglomeration of particles. To counter this, the liquid is heated above the melting point, then cooled to a semi-solid state. Reinforcement particles are preheated before addition to the slurry. The mixture is reheated with stirring until it returns to its initial state before cooling [29, 30].

3.2. Hardness Test

Hardness tests were performed on the matrix (AA5052) and on the matrix reinforced with Al_2O_3 , followed by bauxite. The samples were tested using the same mechanism and under identical working conditions. Multiple readings were taken, and the average was calculated, as shown in Figure 14. A structure that is more uniform and refined, indicating obstruction to dendrites, typically exhibits higher hardness. Reduced grain size contributes to increased strength and hardness, as smaller grain sizes impede dislocation movement by acting as barriers. Furthermore, regions characterized by smaller grain sizes demonstrate elevated hardness, as evident in Figure 15(C). Therefore, the reduction in porosity through enhanced wettability and the uniform distribution of reinforcement particles contribute to increased hardness.

Additionally, grain refinement and improved resistance to cracking or dislocation during hardness tests lead to enhanced hardness. The Brinell hardness results for alloy 5052 with the addition of Al_2O_3 and bauxite are presented in Figure 15. The impact of the addition is evident; under the same conditions, a noticeable difference in hardness is observed between the base material and the composite materials. Thus, the matrix measures 59.1 HB in Figure 15(A), while Figures 15 (B and C) exhibit similar hardness values of 87.5 HB with alumina and 92.3 HB with bauxite, respectively. The results of the hardness test indicate a comparable improvement between alumina and bauxite, with a slight advantage for bauxite. The reason for the slight increase in hardness with bauxite was due to the presence of other elements such as (Ti, Fe and Zn) in addition to alumina. Thus, the presence of these elements improved the structure and makes it more resistant to the penetration of the test ball, then increases the hardness.

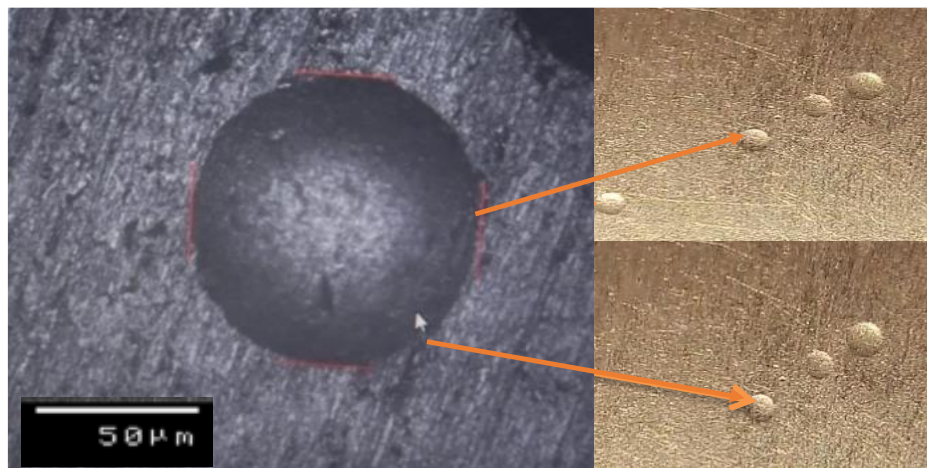


Figure 14. Brinell hardness test.

Furthermore, there was a 48% improvement when alumina reinforced alloy 5052, and a 56% improvement was observed with the addition of bauxite. This enhancement can be attributed to the composite material reinforced with bauxite being free of porosity and more cohesive, as discussed in section 3.1.1.

This implies that the bauxite exhibits more effectiveness than alumina in enhancing hardness, with the same addition percentage (7 wt.%) and under similar working conditions. The effectiveness of bauxite is attributed to its ability to break dendrites, leading to an improved structure after thermal homogenization at 500°C. This outcome can be attributed to bauxite containing a significant amount of alumina, along with other elements that contribute to the enhancement in hardness.

3.3. Wear rate test

Figure 16 (a, b, and c) illustrates the effect of pin sliding on the surface of the alloy samples and the composite materials from two groups, reinforced by alumina and bauxite, respectively. The surface state of the samples is observed after examination conducted under identical working conditions for all samples.

The surface of alloy (a) exhibits more pin penetration compared to (b and c), attributed to the frictional resistance offered by the ceramic reinforcements. Thus, it is clear with an SEM test of the composite sample's surface after performing the wear resistance test, Figure 17.

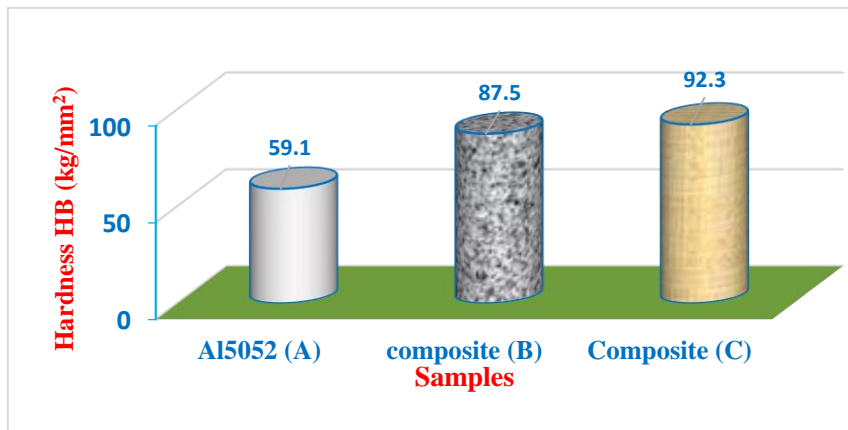


Figure 15. Hardness Comparison tests between: base Alloy 5052 (A) vs. Alloy 5052 with Alumina (B) and Bauxite (C) reinforcements.



Figure 16. Effect of wear test relative to: (a) AA5052, (b) AA5052 reinforced with alumina and (c) AA5052 reinforced with bauxite.

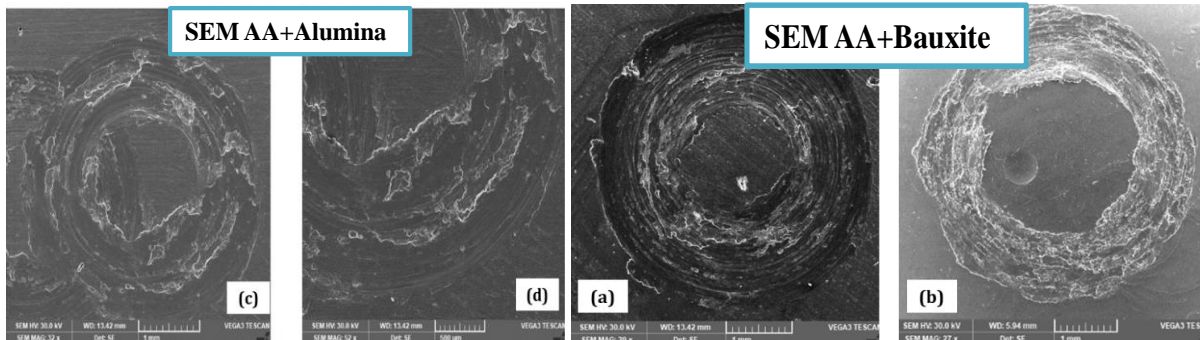


Figure 17. SEM samples images of AA5052+ Al₂O₃ and AA5052+Bauxite

Additionally, it is evident that the surface of (c) is more uniform than (a and b), likely due to bauxite containing elements that enhance the microstructure of the sample. Generally, surfaces reinforced with ceramic materials (b and c) demonstrate resistance to sliding friction from the circular pin movement. This resistance is reflected in the reduced penetration of the pin into these surfaces, indicating the effectiveness of the ceramic particles in resisting friction. The weights before and after operation, and weight loss of the samples for the three time periods (10, 20 and 30 minutes) are shown in Table 6.

Thus, wear rate (WR) was calculated according to the equation $(WR=DW1/S1)$, (S1) represent the sliding distance, that take from the device was 141.056 at (10 minutes), the result of wear rate is (3.757×10^{-5}) , the distant as shown in Figure 18.

Figure 19 illustrates the wear rate on samples of the base alloy and composite materials with the additions of alumina and bauxite. The impact of the ceramic particle additions as reinforcements is evident in the wear rate values, which exhibits a clear decrease with the introduction of these materials.

Table 6. weights before and after operation, and weight loss for all periods

Samples	Initial Weight(g) WO	Weight(g) W1 at 10min.	Weight(g) W2 at 20min.	Weight(g) W3 at 30min.	DW1 WO-W1	DW2 W1-W2	DW3 W2-W3
AA5052	4.7496	4.7443	4.7317	4.7063	0.0053	0.0126	0.0254
AA+Al ₂ O ₃	4.3597	4.3573	4.3515	4.3408	0.0024	0.0059	0.0107
AA+Bauxite	5.0276	5.0251	5.0194	5.0078	0.0025	0.0057	0.0116

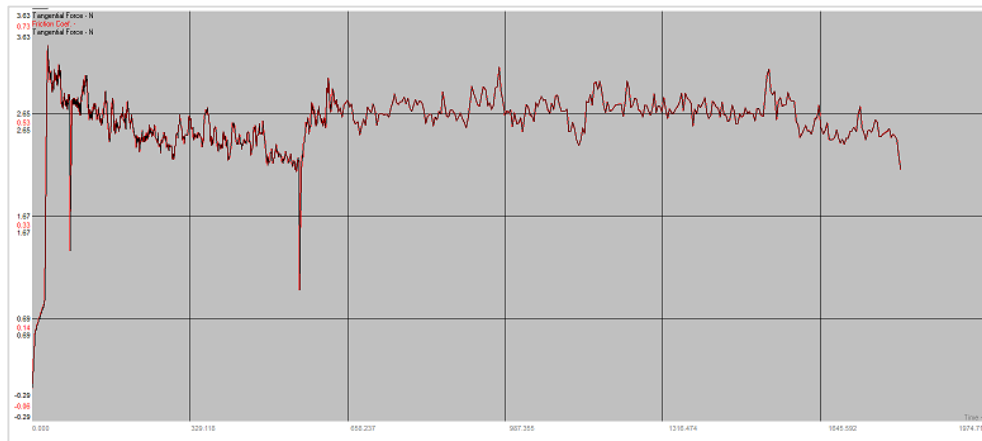


Figure 18. The sliding distance

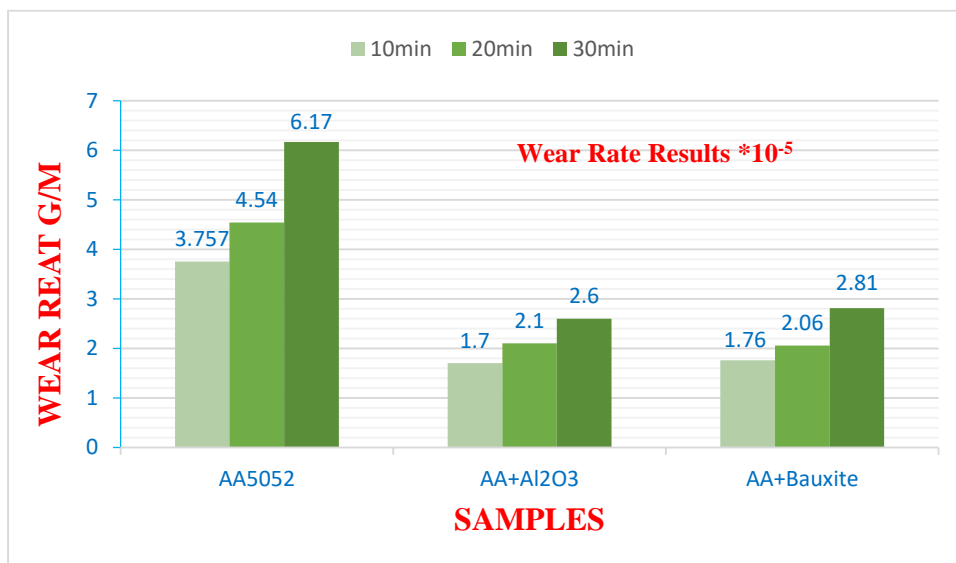


Figure 19. Wear rate comparison: base alloy vs. alloy with alumina and bauxite reinforcements.

For instance, at the ten-minute mark, the wear rate for the base alloy was 3.76×10^{-5} gram per meter (g/m), and this declined to 1.7×10^{-5} and 1.76×10^{-5} g/m with the addition of alumina and bauxite, respectively. Furthermore, the improvement in wear resistance with the addition of alumina and bauxite is notable, with a wear rate decrease of 55% and 53.2%, respectively, at the ten-minute mark. However, the wear rate increases at 20 minutes, reaching 2.1 and 2.06, respectively, with alumina and bauxite. Then, the wear rate increases at 30 minutes, reaching 2.6 and 2.81, respectively, with alumina and bauxite. The enhancement in wear resistance is attributed to the addition of reinforcement ceramic particles. Which refine the grain size and improve mechanical properties, as explained in previous sections.

Wear resistance experiences an increase with the rise in the percentage of reinforcement, attributed to the elevated rigidity and strength, achieved at higher reinforcement levels [30]. Aluminum matrix composite materials incorporating ceramic particles have demonstrated favorable properties, including corrosion resistance, tensile strength, hardness, and impact resistance. The wear resistance shows improvement with both increased particle size and percentage of composite content. Strengthening the aluminum matrix with ceramic particles yields notable improvements in mechanical properties, including enhanced wear resistance, hardness, compressive strength, bending strength, and tensile strength. The extent of improvement varies according to specific applications [31, 32].

4. Conclusion

In the current study, three groups of samples are fabricated by; aluminum alloy AA5052. Then the same alloy reinforced with 7wt% aluminum oxide and lastly the same alloy reinforced with 7wt% natural ceramics (bauxite), where it can be listed the following findings;

- The SEM test showed an improvement in the structure after adding reinforcements, through grains uniform distribution and reduced dendritic branches. Furthermore, the EDS test confirmed the presence of all the added materials. Hence, this was supported by the XRD test, which shows all the elements contained in these materials.
- The effect of alumina and bauxite additions as reinforcements in alloy (AA5052) is apparent in both hardness and wear rate. The hardness improvement reached (87.5 HB and 92.3 HB) with AL₂O₃ and bauxite as reinforcements, respectively. While the wear rate becomes (55.3% and 53.2%) at 10 minutes, (54% and 54.6%) at 20 minutes and (58% and 54.5%) at 30 minutes, with AL₂O₃ and bauxite, respectively.
- The results showed that the current work led to obtaining a composite material with good specifications and economic feasibility in terms of matrices and reinforcement. It can be concluded that the bauxite can be replaced with advanced synthetic ceramic materials at a lower economic cost.

Author contribution

All authors contributed to the research, writing, and reviewing of the paper.

Declarations

Funding: Not applicable.

Ethics approval: Not applicable.

Consent to participate: Not applicable.

Consent for publication: The authors give all the rights to publish the material presented in this work.

Competing interests: The authors declare no competing interests.

References

- [1] S. B. Boppana, S. Dayanand, M. R. A. Kumar, V. Aravinda, "Synthesis and characterization of nano graphene and ZrO₂ reinforced Al 6061 metal matrix composites", *Journal of Materials Research and Technology*, Vol. 9, No. 4, 2020, pp. 7354–7362.
- [2] J. Singh, A. Chauhan, "Characterization of hybrid aluminum matrix composites for advanced applications—A review", *Journal of Materials Research and Technology*, Vol. 5, No. 2, 2016, pp. 159–169. <http://dx.doi.org/10.1016/j.jmrt.2015.05.004>.
- [3] S. Capuzzi, G. Timelli, "Preparation and Melting of Scrap in Aluminum Recycling: A Review," *Metals*, Vol. 8, No.4, 2019, pp. 249. doi:10.3390/met8040249.
- [4] H. Khaireez, Y.N. Kamilah, H. Ariffin, E. Nasha, "Sustainable Aluminum Recycling Method. *Journal of Multi-Disciplinary Engineering Reviews*, Vol. 1, No. 1, 2024, pp. 8-19. <https://doi.org/10.30880/jmer.2024.01.01.002>.
- [5] F. Sheikh Aamir, M. Sheikh Haris, R. Ankush, et al, "Effect of TiB₂ on the mechanical and tribological properties of marine grade Aluminum Alloy 5052: An experimental investigation", *Journal of Materials Research and Technology*, Vol. 29, 2024, pp. 3749-3758.
- [6] A. Mohammed, F. OtonyeTekena, N. Tauqir, "Prediction of Springback Behavior of Vee Bending Process of AA5052 Aluminum Alloy Sheets Using Machine Learning", *Jordan Journal of Mechanical and Industrial Engineering*, Vol. 17, No.1, 2023. <https://doi.org/10.59038/jjmie/170101>.
- [7] Y. M. Almaetah, K. N. Abushgair, M. A. Hamdan, "Aluminium Alloys Nanostructures Produced by Accumulative Roll Bonding (ARB)", *Jordan Journal of Mechanical and Industrial Engineering*, Vol. 15. No.4, 2021.
- [8] A. Abdallah, E.A, El-Danaf, A. Abdulhakim, "The Effect of Alloying, Processing and Heat Treatment on the Wear Resistance of Al-Cu-Mg-Ag Alloys", *Jordan Journal of Mechanical and Industrial Engineering*, 2023, Vol. 17, No. 2, 2023.
- [9] K. Aithal, N. Ramesh Babu, H. N. Manjunath, K. S. Chethan, "Characterization of Al-SiCP Functionally Graded Metal Matrix Composites Developed through Centrifuge Casting Technique", *Jordan Journal of Mechanical and Industrial Engineering*, Vol. 15, No. 5, 2021.
- [10] B. A. Kumar, M. M. Krishnan, A. F. Sahayaraj, M. R. A. Refaai, G. Yuvaraj, D. Madhesh, H. L. Allasi, "Characterization of the aluminium matrix composite reinforced with silicon nitride (AA6061/Si₃N₄) synthesized by the stir casting route", *Advances in Materials Science and Engineering*, Vol. 2022, No.1, 2022, pp. 1–8.
- [11] M. S. Fuhaid, P. K. Krishnan, M. A. Maleque, R. V. Murali, M. Y. Ali, "Manufacturing and Friction Welding of Aluminium Matrix Composites—Review of Current Status

- and Future Directions", *Test Engineering and Management*, pp. 1122–1130, 2020.
- [12] M. Meignanamoorthy, V. Mohanavel, P. Velmurugan, W. B. Alonazi, S. Sivakumar, A. M. Gebrekidan, "Effect of nanoaluminium nitride ceramic particles on microstructure, mechanical wear, and machining behavior of Al-Si-Mg alloy matrix composites produced by bottom pouring type stir casting route", *Journal of Nanomaterials*, Vol. 2022, No.1, 2022, pp. 5013914.
- [13] P. Samal and P. R. Vundavilli, "Investigation of impact performance of aluminum metal matrix composites by stir casting", in *IOP Conference Series: Materials Science and Engineering*, IOP Publishing, 2019, pp. 12047.
- [14] M. Patel, S. K. Sahu, M. K. Singh, N. Dalai, "Micro-structural and mechanical characterization of stir cast AA5052/B₄C metal matrix composite" *Materials Today: Proceedings*, Vol.56, No.3, 2022, pp.1129-1136. <https://doi.org/10.1016/j.matpr.2021.10.331>.
- [15] M. Patel, S. K. Sahu, M. K. D.P. Singh, "Investigation of tribological properties of cast AA5052/B₄C MMC under different loads", *Journal of Tribology*, Vol. 34, 2022, pp. 69–86.
- [16] B. Gugulothu, S. L. Sankar, S. Vijayakumar, A. S. V. Prasad, M. Thangaraj, M. Venkatachalapathy, T. J. Rao, "Analysis of wear behaviour of AA5052 alloy composites by addition alumina with zirconium dioxide using the Taguchi-grey relational method", *Adv. Mater. Sci. Eng.*, Vol. 2022, No.1., 2022, pp. 4545531.
- [17] E. W. A. Fanani, E. Surojo, A. R. Prabowo, D. Ariawan, H. I. Akbar, "Recent development in aluminum matrix composite forging: effect on the mechanical and physical properties", *Procedia Structural Integrity*, Vol. 33, pp. 3–10, 2021.
- [18] S. P. Dwivedi, R. & Sahu, "Effects of SiC Particles Parameters on the Corrosion Protection of Aluminum-based Metal Matrix Composites using Response Surface Methodology". *Jordan Journal of Mechanical and Industrial Engineering*, Vol. 12, No.4, 2018.
- [19] Y. Liu, L. He, S. Yuan, "Wear Properties of Aluminum Alloy 211z. 1 Drilling Tool", *Jordan Journal of Mechanical and Industrial Engineering*, Vol. 15, No.1 2021.
- [20] A. R. I. Kheder, G. S. Marahleh, D. M. K. Al-Jamea, "Strengthening of Aluminum by SiC, Al₂O₃ and MgO", *Jordan Journal of Mechanical and Industrial Engineering*, Vol. 5, No. 6, 2011.
- [21] S. A. Zaidan, M. H. Omar, "The effects of bauxite, metakaolin, and porosity on the thermal properties of prepared Iraqi clays refractory mortars", *Applied Physics A*, Vol. 124, No. 5, 2018. pp. 386.
- [22] A. I. Arogundade, P. S. M. Megat-Yusoff, F. Ahmad *et al.*, "Modification of bauxite residue with oxalic acid for improved performance in intumescent coatings", *Journal of Materials Research and Technology*, Vol. 12, 2021, pp. 679–687.
- [23] M. A. Aswad, S. H. Awad, A. H. Kaayem, "Study on Iraqi Bauxite ceramic reinforced aluminum metal matrix composite synthesized by stir casting", *International Journal of Engineering*, Vol. 33, No. 7, 2020, pp. 1331–1339. doi: 10.5829/IJE.2020.33.07A.20.
- [24] A. S. Verma, M. S. Cheema, S. Kant, N. M. Suri, "Porosity study of developed Al–Mg–Si/bauxite residue metal matrix composite using advanced stir casting process", *Arabian Journal for Science and Engineering*, Vol. 44, 2019, pp.1543-1552.
- [25] K. C. Anil, J. Kumaraswamy, M. Reddy, B. Prakash, "Mechanical behaviour and fractured surface analysis of bauxite residue and graphite reinforced aluminium hybrid composites", *Frattura ed Integrità Strutturale*, Vol. 16, No. 62, 2022, pp. 168-179.
- [26] P. Sharma, S. Sharma, and D. Khanduja, "Production and some properties of Si₃N₄ reinforced aluminium alloy composites", *Journal of Asian ceramic societies*, Vol. 3, No. 3, 2015, pp. 352–359.
- [27] S. Bhaskar, M. Kumar, A. Patnaik, "Mechanical and Tribological overview of ceramic particulates reinforced aluminium alloy composites", *Reviews on Advanced Materials Science*, Vol. 58, No. 1, 2019, pp. 280–294.
- [28] O. Gurumurthy, S. Venkateswaranb, "Experimental Studies and Regression analysis on microstructure and wear loss of MMCs based Zinc-Aluminium alloys with graphite particles reinforcement", *NVEO-NATURAL VOLATILES Essent. OILS Journal| NVEO*, 2021, pp. 1704–1713.
- [29] M. A. A. Al-Jaafari, "Study the effects of titanium dioxide nano particles reinforcement on the mechanical properties of aluminum alloys composite", in *IOP Conference Series: Materials Science and Engineering*, IOP Publishing, 2021, pp. 12062.
- [30] S. Kant and A. S. Verma, "Stir casting process in particulate aluminium metal matrix composite: a review", *International Journal of Mechanics and Solids*, Vol. 9, No. 1, 2017, pp. 61–69.
- [31] T. Sathish, S. Saravanan, and V. Vijayan, "Effect of reinforced aluminium alloy LM30 with pure ceramic particles to evaluate hardness and wear properties", *Material Research Innovation*, Vol. 24, No. 3, 2020, pp. 129–132.
- [32] H. Gowda, & HN. Reddappa "Study on Strontium and Sodium Modification Elements on Microstructure, Mechanical, Wear and Fracture Behavior of Al7075 Alloy by Taguchi, Vol. 18, No 1, 2024.